



ChemComm

**Circularly polarized phosphorescence with large
dissymmetry factor from a helical platinum(II) complex**

Journal:	<i>ChemComm</i>
Manuscript ID	CC-COM-12-2023-006293.R1
Article Type:	Communication

SCHOLARONE™
Manuscripts

COMMUNICATION

Circularly polarized phosphorescence with large dissymmetry factor from a helical platinum(II) complex

Received 00th January 20xx,
Accepted 00th January 20xx

Masahiro Ikeshita,^{‡*a} Shinya Watanabe,^{‡a} Seika Suzuki,^b Shota Tanaka,^c Shingo Hattori,^c Kazuteru Shinozaki,^c Yoshitane Imai^{*b} and Takashi Tsuno^{*a}

DOI: 10.1039/x0xx00000x

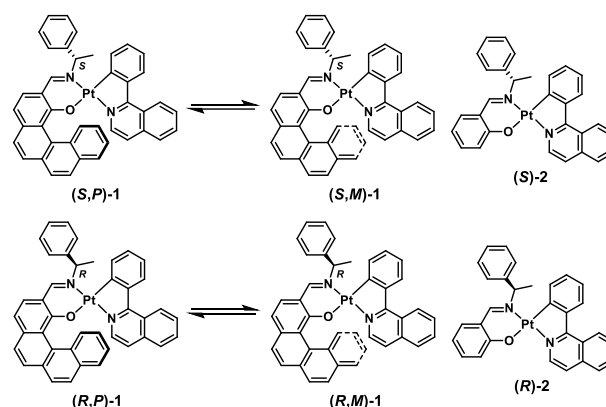
A chiral platinum(II) complex with a helical Schiff-base [4]helicene ligand exhibits intense red circularly polarized phosphorescence (CPP) with a g_{lum} of 0.010 in the dilute solution state. The intense CPP was caused by a change in the transition character based on the induction of the helical backbone.

Chiral materials which exhibit circularly polarized phosphorescence (CPP) have been attracting considerable interest in recent years because of their potential application for circularly polarized organic light-emitting diodes (CP-OLEDs).^{1–3} Square planar platinum(II) complexes are widely known for their highly efficient phosphorescent emission, and CPP materials have been created by introducing chiral ligands.^{4–15} Several chiral platinum(II) complexes have been reported to show CPP with large dissymmetry factors ($g_{\text{lum}} = 2\Delta I/I = 2(I_L - I_R)/(I_L + I_R)$)¹⁸ in the aggregated state.^{7,8,12,16} In particular, the co-assembly of achiral and chiral platinum complexes reported by You and coworkers showed considerably large g_{lum} value of 0.064 from magnetically-allowed metal-metal-to-ligand charge transfer (MMLCT) transition.⁸ However, in the solution-dispersed state, the CPP intensities are low for most of the platinum(II) complexes, usually on the order of 10^{-3} .^{6,9,12–15} This is because platinum complexes usually exhibit magnetically forbidden metal-to-ligand charge transfer (MLCT)-derived phosphorescence.

Helicenes represent a group of compounds in which aromatic rings are helically fused, and are known to exhibit strong chiroptical properties based on their specific helical chirality.^{19–21} Furthermore, there have been reports of materials exhibiting highly efficient CPP by introducing helicene ligands

into Pt(II),^{4–6,17} Ir(III),^{22,23} Re(I)^{24,25} and Au(I)²⁶ centres. The most successful example was reported by Autschbach, Crassous and coworkers in which a platinum(II) complex with a [6]helicene framework exhibited CPP of the order of 10^{-2} in the solution-dispersed state at room temperature.^{4,27}

Our research group has been investigating photophysical properties of chiral transition metal complexes and recently found that Schiff-base platinum(II) complexes having distorted square planar coordination platforms exhibit tunable CPP properties in solution,^{11,13,14} in the polymer-dispersed state,¹⁰ and in the solvent-free liquid state.¹² In the present study, we designed a novel chiral platinum complex **1** with a Schiff-base [4]helicene ligand and the photophysical properties of the complex were compared with its analogue **2** (Scheme 1). Single crystal X-ray diffraction (SCXRD) analysis revealed that complex **1** crystallized having a unidirectional helical structure which depends on the chirality of the phenylethyl moiety (*P* chirality for (*S*)-**1** and *M* chirality for (*R*)-**1**). In solution, complex **1** exhibits a diastereomeric equilibrium with helical inversion of the [4]helicene framework, and the ratio of the diastereomers changes with the polarity of the solvent. The intense CPP was observed for helical complex **1**, reaching $g_{\text{lum}} = 0.010$. We performed density functional theory (DFT)



Scheme 1 Structures and diastereomeric equilibrium of helical platinum complex **1** and its analogue **2** studied in this work.

^a Department of Applied Molecular Chemistry, College of Industrial Technology, Nihon University, Narashino, Chiba 275-8575, Japan.

E-mail: ikeshita.masahiro@nihon-u.ac.jp, tsuno.takashi@nihon-u.ac.jp

^b Department of Applied Chemistry, Faculty of Science and Engineering, Kindai University 3-4-1 Kowakae, Higashi-Osaka, Osaka 577-8502, Japan.

E-mail: y-imai@apch.kindai.ac.jp.

^c Graduate School of Nanobioscience, Yokohama City University 22-2 Seto, Kanazawa-ku, Yokohama 236-0027, Japan

Electronic Supplementary Information (ESI) available. See DOI: 10.1039/x0xx00000x

[‡] These authors contributed equally to this work.

calculations to understand the relationships between molecular structures and photophysical properties.

A series of chiral platinum complexes (*R*)-/(*S*)-**1** and (*R*)-/(*S*)-**2** was prepared by reaction of μ -dichloro-bridged dimer [Pt(piq)Cl]₂²⁸ (piq = 1-phenylisoquinoline) with optically pure Schiff-base ligands in boiling dimethyl sulfoxide (DMSO) and toluene. In this reaction, *cis*-isomers were not observed in the reaction mixture and *trans*-isomers were selectively obtained. The newly synthesized complexes **1** and **2** were successfully characterized by infra-red (IR) spectroscopy, ¹H and ¹³C nuclear magnetic resonance (NMR) spectroscopy (Fig. S4 and S5, ESI†), gradient correlation spectroscopy (gCOSY) (Figure S6a, ESI†), nuclear Overhauser effect spectroscopy (NOESY) (Figures S6b, ESI†) and high-resolution mass spectrometry (HRMS).

Single crystals of racemic mixtures of *rac*-**1** and *rac*-**2** were obtained by recrystallization from EtOAc for *rac*-**1** and DMSO for *rac*-**2**, respectively, and employed for SCXRD analysis. Due to the low crystallinity of optically pure complexes, racemic samples were prepared by mixing a 1:1 ratio of (*R*)- and (*S*)-form. ORTEP drawings of complexes (*S*)-**1** and (*S*)-**2** in their racemic crystals are shown in Fig. 1, and the packing structures in the lattice are shown in Fig. S7 and S8. In both complexes, Schiff-base ligands took bent structures, while the piq framework had planar structures. The dihedral angles of the four atoms coordinated to platinum centre (O–N(1)–C–N(2) (ϕ)) are provided to express the degree of distortion of the tetrahedral coordination geometries.²⁹ The ϕ angles of (*S*)-**1** and (*S*)-**2** have the negative values -10.37° and -8.09° , respectively, suggesting that both (*S*)-isomers have Δ configuration in the crystal. Furthermore, complex (*S*)-**1** crystallized having a unidirectional helical structure ((*S,P*)-form) induced by the chirality of the phenylethyl moiety on the nitrogen atom. The sum of the torsion angles θ of the inner rims of the quasi-[5]helicene framework for (*S*)-**1** (from O–C_a–C_b–C_c to C_b–C_c–C_a–C_c) was calculated to be 58.48° , slightly smaller than that of [5]carbohelicene (63.83°).³⁰

We subsequently performed ¹H NMR measurement to investigate the helical inversion behaviour of complex **1**. ¹H NMR spectra of (*S*)-**1** in CDCl₃ show a diastereomeric

equilibrium based on different signals associated with the (*S,P*) and (*S,M*)-diastereomers (Fig. 2a and S9, ESI†). The diastereomeric ratio was estimated to be (*S,P*) : (*S,M*) = 1 : 1 from integration values of the ¹H NMR spectra. On the other hand, the diastereomeric ratio changed in CD₂Cl₂ and DMSO-*d*₆, where the diastereomeric excesses (*de*) were estimated to be 18%*de* for CD₂Cl₂ (Fig. 2b and S9, ESI†) and 33%*de* for DMSO-*d*₆ (Fig. 2c and S10, ESI†), respectively. These results indicate that the polarity of the solvent alters the stability of the diastereomers. Furthermore, racemic single crystals of complex **1** were dissolved in toluene-*d*₈ at 195 K and ¹H NMR measurements were performed at -60°C . Only one diastereomeric signal of (*S,P*)/(*R,M*)-**1** was observed and the signal of (*S,M*)/(*R,P*)-**1** was not detected (Figure S12, ESI†). This result indicates that complex **1** was dissolved in toluene-*d*₈ retaining the structure of the crystalline state at low temperatures. Diastereomeric equilibrium was then observed upon heating, reaching (*S,P*)/(*R,M*) : (*S,M*)/(*R,P*) = 1 : 1 at room temperature.

The UV–vis absorption spectra of complexes (*S*)-**1** and (*S*)-**2** measured in CH₂Cl₂ have a broad absorption band around 400–500 nm that is mainly attributable to the mixture of MLCT and ligand-to-ligand charge transfer (LLCT) (Fig. 3 upper figure). The assignment of transition characters of the absorption band will be discussed in a later section on DFT calculations. The CD spectra of complexes **1** and **2** were measured under the same conditions as the UV–vis absorption spectra (Fig. 3 lower figure). Complexes (*S*)-**1** and (*S*)-**2** exhibited positive Cotton effects in the range of 400–500 nm, which can be assigned to the mixture of MLCT/LLCT transitions of the UV–vis spectra in the same region. The g_{abs} (= $\Delta\epsilon/\epsilon$) values around the absorption maxima in the low energy region are -2.6×10^{-4} (481 nm) for (*S*)-**1** and -2.2×10^{-4} (460 nm) for (*S*)-**2**, respectively. CD spectra of complexes **1** were also recorded in CDCl₃ and DMSO-*d*₆ (Fig. S13, ESI†). The CD patterns differed depending on the solvent, which can be attributed to changes in the diastereomeric ratio observed by the ¹H NMR spectra.

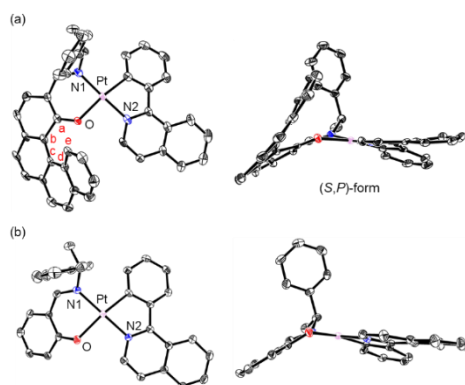


Fig. 1 ORTEP drawings of (a) (*S*)-**1** and (b) (*S*)-**2** in the racemic crystals. Thermal ellipsoids are shown at the 50% probability level. Hydrogen atoms and solvent molecules are omitted for clarity.

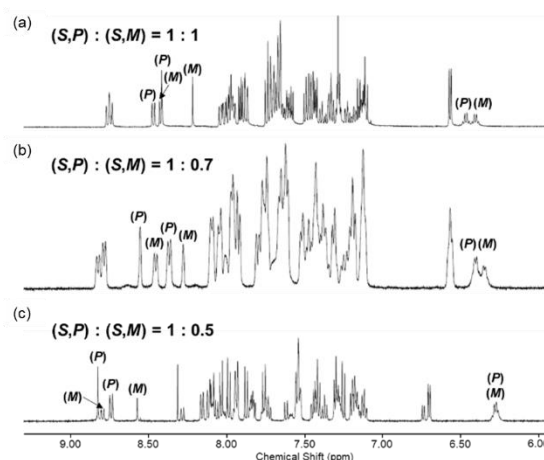


Fig. 2 ¹H NMR spectra of (*S*)-**1** in (a) CDCl₃, (b) CD₂Cl₂ and (c) DMSO-*d*₆ in the aromatic region (500 MHz, 298 K).

Complexes **1** and **2** exhibited red photoluminescence under UV excitation at room temperature in CH₂Cl₂ (Fig. 4 inset of lower figures). Details of the photophysical properties are summarised in Table S2. The emission lifetimes of the complexes were determined to be $\tau = 0.21 \mu\text{s}$ for (*S*)-**1** and $\tau = 0.13, 2.3 \mu\text{s}$ (94:6) for (*S*)-**2**, respectively, suggesting that the emissions from (*S*)-**1** and (*S*)-**2** are phosphorescence (Figure S14, ESI†). The circularly polarized luminescence (CPL) and total luminescence spectra measured for complexes **1** and **2** in CH₂Cl₂ solution at 298 K are shown in Fig. 4. The CPL spectra of **1** and **2** having opposite (*R*)- and (*S*)-configurations exhibit mirror-image signals around 608 nm (Fig. 4 upper figures), which are corresponding to the emission peak maxima (λ_{max}) observed in their total emission spectra (Fig. 4 lower figures). The CPL signs were inverted between the two complexes, which was positive in (*S*)-**1** and negative in (*S*)-**2**. The g_{lum} values were calculated as the average of three points including λ_{max} and estimated to be 0.010 for (*S*)-**1** and 0.003 for (*S*)-**2**, respectively. Brightness for CPL ($B_{\text{CPL}} = (\epsilon \times \Phi \times g_{\text{lum}})/2$) were also calculated to be $1.1 \text{ M}^{-1} \text{ cm}^{-1}$ for (*S*)-**1** and $0.3 \text{ M}^{-1} \text{ cm}^{-1}$

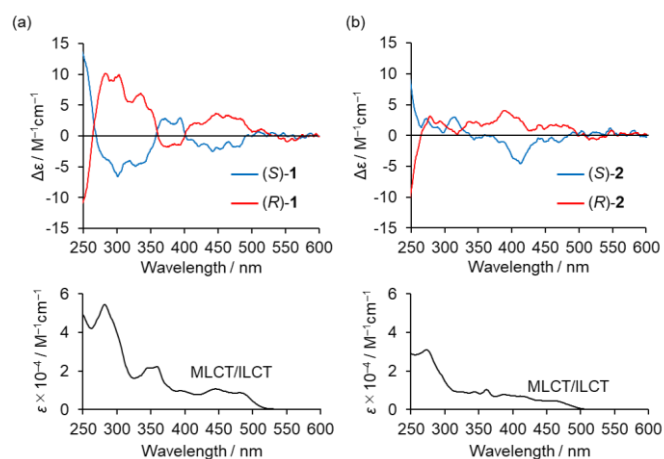


Fig. 3 UV-vis (upper plot) and CD (lower plot) spectra of $2.0 \times 10^{-4} \text{ M}$ solutions of (a) **1** and (b) **2** in CH₂Cl₂ at 298 K.

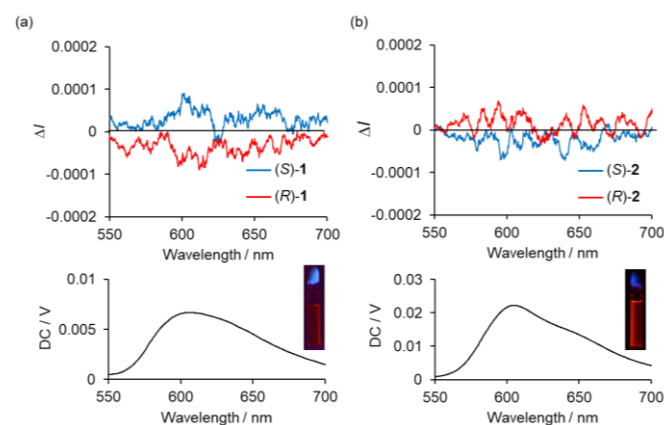


Fig. 4 CPL (upper plot) and total emission (lower plot) spectra of $2.0 \times 10^{-4} \text{ M}$ solutions of (*R*)- and (*S*)- (a) **1** and (b) **2** in CH₂Cl₂ at 298 K ($\lambda_{\text{ex}} = 480 \text{ nm}$ (**1**) and 470 nm (**2**)). The insets in the lower figure show the photographs under UV irradiation.

for (*S*)-**2**, respectively, which is moderate value among the CPP-active platinum(II) complexes.³¹

To consider the photophysical properties of the platinum complexes, we performed DFT calculations on the B3LYP/6-31+G(d,p), LanL2DZ level, using the Gaussian 16 program. The structures of (*S,P*)-**1** and (*S*)-**2** were optimized from the results of SCXRD structures. To obtain optimized structures of (*S,M*)-**1**, we inverted the configuration of optimized (*S,P*)-**1** structure and repeated the optimization procedure. The HOMOs of the both complexes consist of the hybrids of the d_{xz} orbital of the platinum centre and the π -orbitals of the Schiff-base ligands, whereas the LUMOs are in the π^* orbitals of piq frameworks (Figure S16 and S17, ESI†). The major electronic configurations of the S_1 states were HOMO-to-LUMO transitions, which implies that the absorption bands observed in the visible region can be attributed to the mixture of ¹MLCT/¹LLCT transitions (Tables S3, ESI†). Electrostatic potential (ESP) surfaces and dipole moments in the S_0 optimized state were also calculated and results were shown in Fig. S20. (*S,P*)-**1** has a larger dipole moment than (*S,M*)-**1**, suggesting that (*S,P*)-**1** is stabilized by solvation in polar solvents and exhibits higher d_e values. In the case of CDCl₃ solution, the trace amount of acid in the solvent may have reduced the difference in the stability of the diastereomers.

Simulated CD spectra of the complexes (*S,P*)-**1**, (*S,M*)-**1** and (*S*)-**2** are shown in Fig. S21. Opposite handedness signals were observed in the visible region of the diastereomers (*S,P*)-**1** and (*S,M*)-**1**. Since the two diastereomers are in equilibrium in solution, the experimental CD spectrum is considered to be a mixture of these diastereomeric spectra. Furthermore, (*S*)-**2** has a weaker CD signal than **1**. The theoretical g_{abs} values of $S_0 \rightarrow S_1$ transition were estimated to be 1.7×10^{-3} for (*S,P*)-**1**, -1.9×10^{-3} for (*S,M*)-**1** and -5.3×10^{-4} for (*S*)-**2**, respectively (Figure S21). These results suggest that the [4]helicene framework contributes to the enhanced chiroptical properties. Although the CPL sign inversion between **1** and **2** is still unclear, we assume that the CPL sign of **1** depends on the helicity of [4]helicene framework as well as $S_0 \rightarrow S_1$ transition calculated for CD spectra.

Finally, in order to further characterize the phosphorescence nature of complexes **1** and **2**, we performed a natural transition orbital (NTO) analysis³² on the basis of T_1 optimized geometries (Fig. 5). The NTO holes reside $d-\pi$ hybrids of the platinum atom and the Schiff-base ligands in both complexes. On the other hand, the NTO particles of (*S,P*)-**1** and (*S,M*)-**1** extend to the whole molecule including the [4]helicene backbone, while that of (*S*)-**2** localized to the piq framework. Therefore, in the phosphorescence of complex **1**, there is also a contribution of the intra-ligand charge transfer (ILCT) character of the [4]helicene backbone. These results suggest that the high g_{lum} value of complex **1** is due to the extension of the transition density over the whole molecule.³³

In summary, we have developed a helical platinum(II) complex with a chiral Schiff-base [4]helicene ligand. The complex exhibits intense red CPP in dilute solution. Notably, the g_{lum} value of the complex was calculated to be 0.010 which is a quite high value for small organic and organometallic

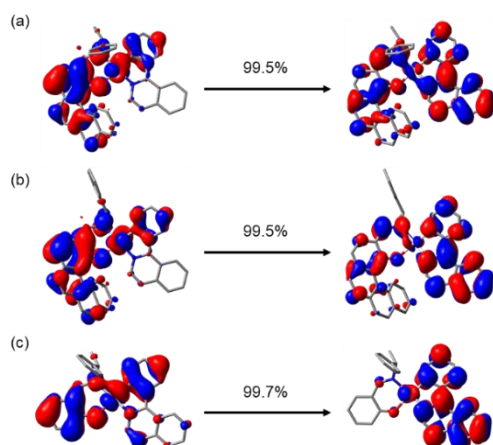


Fig. 5 NTO analysis of the $S_0 \rightarrow T_1$ transition for (a) (S,P)-1, (b) (S,M)-1 and (c) (S)-2 as obtained from DFT calculations (B3LYP/6-31G*, LanL2DZ).

materials. A comparison with complexes without helical structure revealed that the ILCT character of the [4]helicene ligand in the $S_0 \rightarrow T_1$ transition is the key to increasing the g_{lum} value. Researches are currently underway to consider the CPP intensity from the viewpoint of transition dipole moments and to design CPP materials with g_{lum} exceeding 10^{-1} .

This work was supported by JSPS KAKENHI (Grant Numbers JP23K13768 (M.I.), JP21K14647 (S.H.), JP23H02040 (Y.I.) and JP21K05234 (T.T.)), JST, CREST (Grant Number JPMJCR2001 (Y.I.)), the Sasakawa Scientific Research Grant from The Japan Science Society (M.I.) and Nihon University Industrial Technology Fund for Supporting Young Scholars (M.I.). We gratefully acknowledge Prof. Dr. Henri Brunner (Universität Regensburg) for helpful discussion, Prof. Dr. Takayoshi Fujii (Nihon University) for emission measurements and Assoc. Prof. Dr. Shuichi Suzuki (Osaka University) for measurements of HRMS spectrometry.

Conflicts of interest

There are no conflicts to declare.

Notes and references

- 1 Y.-P. Zhang and Y.-X. Zheng, *Dalton Trans.*, 2022, **51**, 9966.
- 2 Z.-L. Gong, Z.-Q. Li and Y.-W. Zhong, *Aggregate*, 2022, **3**, e177.
- 3 X. Wang, S. Ma, B. Zhao and J. Deng, *Adv. Funct. Mater.*, 2023, **33**, 2214364.
- 4 (a) C. Shen, E. Anger, M. Srebro, N. Vanthuyne, K. K. Deol, T. D. Jefferson, G. Muller, J. A. G. Williams, L. Toupet, C. Roussel, J. Autschbach, R. Réau and J. Crassous, *Chem. Sci.*, 2014, **5**, 1915; (b) H. D. Ludowing, M. Srebro-Hooper, J. Crassous, J. Autschbach, *ChemistryOpen*, 2022, **11**, e202200020.
- 5 J. R. Brandt, X. Wang, Y. Yang, A. J. Campbell and M. J. Fuchter, *J. Am. Chem. Soc.*, 2016, **138**, 9743.
- 6 T. Biet, T. Cauchy, Q. Sun, J. Ding, A. Hauser, P. Oulevey, T. Bürgi, D. Jacquemin, N. Vanthuyne, J. Crassous and N. Avarvari, *Chem. Commun.*, 2017, **53**, 9210.
- 7 J. Song, M. Wang, X. Zhou and H. Xiang, *Chem. – Eur. J.*, 2018, **24**, 7128.
- 8 G. Park, H. Kim, H. Yang, K. R. Park, I. Song, J. H. Oh, C. Kim and Y. You, *Chem. Sci.*, 2019, **10**, 1294.
- 9 R. Inoue, R. Kondo and Y. Morisaki, *Chem. Commun.*, 2020, **56**, 15438.
- 10 M. Ikeshita, S. Furukawa, T. Ishikawa, K. Matsudaira, Y. Imai and T. Tsuno, *ChemistryOpen*, 2022, **11**, e202100277.
- 11 M. Ikeshita, T. Yamamoto, S. Watanabe, M. Kitahara, Y. Imai and T. Tsuno, *Chem. Lett.*, 2022, **51**, 832.
- 12 M. Ikeshita, K. Orioku, K. Matsudaira, M. Kitahara, Y. Imai and T. Tsuno, *ChemPhotoChem*, 2023, **7**, e202300010.
- 13 M. Ikeshita, Y. Tani, M. Kitahara, Y. Imai and T. Tsuno, *Bull. Chem. Soc. Jpn.*, 2023, **96**, 969.
- 14 M. Ikeshita, N. Hara, Y. Imai and T. Naota, *Inorg. Chem.*, 2023, **62**, 13964.
- 15 J. Song, H. Xiao, B. Zhang, L. Qu, X. Zhou, P. Hu, Z.-X. Xu and H. Xiang, *Angew. Chem., Int. Ed.*, 2023, **62**, e202302011.
- 16 D. Tauchi, T. Koida, Y. Nojima, M. Hasegawa, Y. Miyazaki, A. Inagaki, K. Sugiura, Y. Nagaya, K. Tsubaki, T. Shiga, Y. Nagata and H. Nishikawa, *Chem. Commun.*, 2023, **59**, 4004.
- 17 D. Kundu, N. del Rio, M. Cordier, N. Vanthuyne, E. V. Puttock, S. C. J. Meskers, J. A. G. Williams, M. Srebro-Hooper and J. Crassous, *Dalton Trans.*, 2023, **52**, 6484.
- 18 H. Tanaka, Y. Inoue and T. Mori, *ChemPhotoChem*, 2018, **2**, 386.
- 19 Y. Shen and C.-F. Chen, *Chem. Rev.*, 2012, **112**, 1463.
- 20 W.-L. Zhao, M. Li, H.-Y. Lu and C.-F. Chen, *Chem. Commun.*, 2019, **55**, 13793.
- 21 K. Dhbaibi, L. Favereau, J. Crassous, *Chem. Rev.*, 2019, **119**, 8846.
- 22 N. Hellou, M. Srebro-Hooper, L. Favereau, F. Zinna, E. Caytan, L. Toupet, V. Dorcet, M. Jean, N. Vanthuyne, J. A. G. Williams, L. Di Bari, J. Autschbach and J. Crassous, *Angew. Chem., Int. Ed.*, 2017, **56**, 8236.
- 23 E. S. Gauthier, N. Hellou, E. Caytan, S. D. Fré, V. Dorcet, N. Vanthuyne, L. Favereau, M. Srebro-Hooper, J. A. G. Williams and J. Crassous, *Inorg. Chem. Front.*, 2021, **8**, 3916.
- 24 E. S. Gauthier, L. Abella, N. Hellou, B. Darquité, E. Caytan, T. Roisnel, N. Vanthuyne, L. Favereau, M. Srebro-Hooper, J. A. G. Williams, J. Autschbach and J. Crassous, *Angew. Chem., Int. Ed.*, 2020, **59**, 8394.
- 25 E. S. Gauthier, L. Abella, E. Caytan, T. Roisnel, N. Vanthuyne, L. Favereau, M. Srebro-Hooper, J. A. G. Williams, J. Autschbach and J. Crassous, *Chem. – Eur. J.*, 2023, **29**, e202203477.
- 26 E. S. Gauthier, M. Cordier, V. Dorcet, N. Vanthuyne, L. Favereau, J. A. G. Williams and J. Crassous, *Eur. J. Org. Chem.*, 2021, 4769.
- 27 Recently, the CPL spectra of the [6]helicene platinum complexes were re-measured by the authors. They conclude that a more realistic g_{lum} value of 3×10^{-3} was obtained and was reported. See Ref. 4b.
- 28 D. Kourkoulos, C. Karakus, D. Hertel, R. Alle, S. Schmeding, J. Hummel, N. Risch, E. Holder and K. Meerholz, *Dalton Trans.*, 2013, **42**, 13612.
- 29 H. Brunner, M. Bodensteiner, T. Tsuno, *Chirality* 2013, **25**, 663.
- 30 T. Kaehler, A. John, T. Jin, M. Bolte, H.-W. Lerner and M. Wagner, *Eur. J. Org. Chem.* 2020, 5847.
- 31 L. Arrico, L. Di Bari, F. Zinna, *Chem. Eur. J.*, 2021, **27**, 2920.
- 32 R. L. Martin, *J. Chem. Phys.*, 2003, **118**, 4775.
- 33 Z. Chen, M. Huang, C. Zhong, S. Gong, V. Coropceau, J.-L. Brédas, C. Yang, *Chem. Sci.*, 2023, **14**, 6022.